

Radioluminescent Ionic Liquids: Designer Materials for Detecting and Quantifying Ionizing Radiation

Dario Rodrigues, Gabriela Pabla Sarmiento, Nicolas Ivan Krimer, and Martín Mirenda

ACS Appl. Electron. Mater., **Just Accepted Manuscript** • DOI: 10.1021/acsaelm.0c00523 • Publication Date (Web): 24 Jul 2020

Downloaded from pubs.acs.org on July 25, 2020

Just Accepted

“Just Accepted” manuscripts have been peer-reviewed and accepted for publication. They are posted online prior to technical editing, formatting for publication and author proofing. The American Chemical Society provides “Just Accepted” as a service to the research community to expedite the dissemination of scientific material as soon as possible after acceptance. “Just Accepted” manuscripts appear in full in PDF format accompanied by an HTML abstract. “Just Accepted” manuscripts have been fully peer reviewed, but should not be considered the official version of record. They are citable by the Digital Object Identifier (DOI®). “Just Accepted” is an optional service offered to authors. Therefore, the “Just Accepted” Web site may not include all articles that will be published in the journal. After a manuscript is technically edited and formatted, it will be removed from the “Just Accepted” Web site and published as an ASAP article. Note that technical editing may introduce minor changes to the manuscript text and/or graphics which could affect content, and all legal disclaimers and ethical guidelines that apply to the journal pertain. ACS cannot be held responsible for errors or consequences arising from the use of information contained in these “Just Accepted” manuscripts.

Radioluminescent Ionic Liquids: Designer Materials for Detecting and Quantifying Ionizing Radiation

Dario Rodrigues,^{,†,‡} Gabriela P. Sarmiento,[†] Nicolas I. Krimer,[†] and Martin Mirenda^{*,†}*

[†]Gerencia Química, Centro Atómico Constituyentes, Comisión Nacional de Energía Atómica (CNEA-CONICET), Av. Gral. Paz 1499, B1650KNA San Martín, Buenos Aires, Argentina.

[‡]Departamento de Física, Facultad de Ciencias Exactas y Naturales, Universidad de Buenos Aires, Ciudad Universitaria, Pab. I, C1428EHA, Buenos Aires, Argentina.

KEYWORDS: ionic liquids, radioluminescence, energy transfer, ionizing radiation, scintillation

ABSTRACT: A designed radioluminescent ionic liquid (RadIL), composed of a single imidazolium cation and two different fluorescent anions, is presented. The material allows the conversion of the energy released by energetic charged particles into visible

1
2
3 light by radioluminescence. Its capability in detecting and in quantifying alpha and beta
4
5
6
7 particles was proved by its use as a solvent in liquid scintillation counting. A keynote of
8
9
10 this performance is that its radioluminescence yield strongly depends on temperature.
11
12
13 This feature represents a clear advantage compared with common commercial
14
15
16 scintillators composed of organic volatile solvents that cannot be usually heated. The
17
18
19 temperature dependence of the radioluminescent material allows the disentangling of
20
21
22 the Cherenkov and radioluminescence contributions emerging from samples containing
23
24
25 one or more radionuclides. As such, this property can be used for alpha/beta
26
27
28 quantification in radionuclide mixtures, following a pre-calibration of the material
29
30
31 response to each radionuclide present in the blend. This RadIL represents the first
32
33
34 precedent of an innovative family of luminescent ILs to be developed. The rational
35
36
37 design of these materials opens interesting possibilities of real-time quantifications of
38
39
40 fission products during the reprocessing of spent nuclear fuels.
41
42
43
44
45
46
47
48
49

50 INTRODUCTION

51
52
53
54
55
56
57
58
59
60

1
2
3
4 The last two decades have witnessed a growing interest on the a new class of
5
6
7 versatile organic salts normally referred to as ionic liquids (ILs).¹ These designer
8
9
10 compounds have been proposed for a manifold of applications in different areas of
11
12
13 medicine,² electronics,³ renewable energies,^{4,5} lasers⁶ and nuclear fuel cycle,^{7,8} to cite a
14
15
16 few relevant examples. Usually, they are described as *designer compounds*, since their
17
18
19 anions and cations can be independently tailored for tuning specific physicochemical
20
21
22 properties of interest.^{9,10} Due to their low vapor pressures and low flammability, among
23
24
25 other peculiar characteristics,¹¹ they have been proposed as suitable materials for
26
27
28 actinide ion extraction¹² and nuclear fuel reprocessing.^{13,14} Luminous response to the
29
30
31 presence of radioactive material would be a desirable property to quantify the yield of
32
33
34 such a reprocessing. As such, the discovery of new scintillation compounds with
35
36
37 improved efficiencies represents a continuing challenge.¹⁵
38
39
40
41
42
43
44
45

46 Six years ago it was reported that pure IL 1-butyl-3-methylimidazolium chloride
47
48
49 [BMIm⁺][Cl⁻] IL was able to detect and quantify ionizing radiation by means of
50
51
52 Cherenkov counting.¹⁶ More recently, it was showed that the addition of the wavelength-
53
54
55
56
57
58
59
60

1
2
3 shifter 1-butyl-3-methylimidazolium 8-hydropyren-trisulfonate [BMIm⁺][HPTS³⁻] to
4
5
6
7 [BMIm⁺][Cl⁻] enhances the Cherenkov detection efficiency for the most commonly used
8
9
10 commercial photomultipliers.¹⁷ In what follows, it is presented here an advanced
11
12
13 designed radioluminescent IL (RadIL) that generates luminescence from electronically
14
15
16 excited molecular species after being excited by ionizing radiation. This novel material,
17
18
19 which combines [BMIm⁺] as a common cation and [Cl⁻], [HPTS³⁻] and tosylate [Tos⁻] as
20
21
22 anions, represents the first precedent of an innovative family of ILs with interesting
23
24
25 applications.
26
27
28
29
30
31

32 EXPERIMENTAL SECTION

33
34
35
36

37 *Reagents and synthesis.* [BMIm⁺][Cl⁻] was synthesized and purified as described in a
38
39 previous work.¹⁸ 1-Butyl-3 methylimidazolium 4-toluensulfonate [BMIm⁺][Tos⁻] was
40
41
42 obtained from the [BMIm⁺][Cl⁻] and the 4-toluensulfonic acid sodium salt [Na⁺][Tos⁻] via
43
44
45 a metathesis reaction from the exchange between chloride and [Tos⁻] anions.
46
47
48
49
50
51 [Na⁺][Tos⁻] was previously obtained from neutralization of an aqueous solution of 4-
52
53
54 toluensulfonic acid [H⁺][Tos⁻] monohydrate (Sigma-Aldrich, purity > 98.5%, used as
55
56
57
58
59
60

1
2
3 received) with an aqueous solution of NaOH (sodium hydroxide, Merk, analytical
4
5
6
7 reagent, used as received) and subsequent evaporation. $[\text{Na}^+][\text{Tos}^-]$ was added to a
8
9
10 solution of $[\text{BMIm}^+][\text{Cl}^-]$ in dichloromethane, in a mole proportion of 1.1:1. The later
11
12
13
14 mixture was left under continuous stirring for seven days at room temperature. The
15
16
17 resulting solution was filtered and evaporated under reduced pressure. A metastable
18
19
20 colorless viscous liquid was obtained (mp: 63.9 °C from Differential Scanning
21
22
23 Calorimetry, DSC, see Supporting Information). $^1\text{H-NMR}$: (500 MHz, D_2O , δ in ppm)
24
25
26
27 8.65 (s, 1H), 7.67 (d, 2H, $J = 7.4$ Hz), 7.42 (d, 1H, $J = 1.8$ Hz), 7.38 (d, 1H, $J = 1.8$ Hz),
28
29
30
31 7.35 (d, 2H, $J = 7.4$ Hz), 4.14 (t.n.r., 2H), 3.85 (s, 3H), 2.38 (s, 3H), 1.81 (quin, 2H, $J =$
32
33
34
35 7.4 Hz), 1.29 (sext, 2H, $J = 7.4$ Hz), 0.91 (t, 3H, $J = 7.4$ Hz). (s: singlet; d: doublet, t:
36
37
38 triplet, t.n.r.: triplet not resolved, quin: quintuplet, sext: sextuplet). An 1:1 stoichiometric
39
40
41 ratio between $[\text{BMIm}^+]$ and $[\text{Tos}^-]$ was estimated from the comparison of the hydrogen's
42
43
44
45 integrated areas of both species. A chloride test using a silver nitrate solution showed
46
47
48
49 negative results.
50
51
52
53
54
55
56
57
58
59
60

[BMIm⁺][HPTS³⁻] was synthesized from [BMIm⁺][Cl⁻] and pyranine (8-hydroxypyrene-1,3,6-trisulfonic acid trisodium salt, [Na⁺][HPTS³⁻], Aldrich, purity > 97%, used as received) via a metathesis reaction from the exchange between the chloride and [HPTS³⁻] anions. Solid pyranine was added to a solution of [BMIm⁺][Cl⁻] in dichloromethane (Merk, purity >99.9%, used as received) in a mole proportion of 1:2.7. The reaction mixture was left under continuous stirring for seven days at room temperature. The solution was filtered and then evaporated under reduced pressure. A yellow/brown solid was obtained (mp: 136.3 °C from DSC, see Supporting Information). ¹H -NMR: (500 MHz, D₂O, δ in ppm) 9.03 (s, 1H), 8.95 (d, 1H, J = 9.7 Hz), 8.84 (d, 1H, J = 9.6 Hz), 8.77 (d, 1H, J = 9.7 Hz), 8.53 (d, 1H, J = 9.6 Hz), 8.21 (t.n.r., 1H), 8.17 (s, 1H), 6.96 (t, 1H, J = 1.8 Hz), 6.93 (t, 1H, J = 1.8 Hz), 3.63 (t, 2H, J = 7.4 Hz), 3.56 (s, 3H), 1.37 (quin, 2H, J = 7.4 Hz), 0.96 (sext, 2H, J = 7.4 Hz), 0.64 (t, 3H, J = 7.4 Hz). An 1:3.6 stoichiometric ratio between [HPTS³⁻] and [BMIm⁺] was estimated by comparing the hydrogen's integrated areas of both species. This revealed a remnant of [Cl⁻] anions in the final product, indicating that the metathesis was not complete. Chloride test using a silver nitrate solution showed positive results confirming this issue.

1
2
3 [BMIm⁺][Cl⁻] / [BMIm⁺][Tos⁻] / [BMIm⁺][HPTS³⁻] mixtures were prepared by addition of
4
5
6
7 weighted amounts of the synthesized compounds. The density of all samples was 1.07
8
9
10 g/mL. The samples were heated at 60 °C in a water bath, and mixed during 24 hours
11
12
13 with magnetic stirring to ensure the complete homogenization. Afterward, mixtures were
14
15
16 cooled down to room temperature. The RadIL composition was 2.2×10^{-4} M of
17
18 [BMIm⁺][HPTS³⁻] in a mixture of 36%, in mass, of [BMIm⁺][Cl⁻] and 64% of
19
20
21 [BMIm⁺][Tos⁻].¹⁹ Mixtures obtained without the [BMIm⁺][HPTS³⁻] component, will be
22
23
24 denoted as [BMIm⁺]₂[Cl⁻] [Tos⁻] because they present a mole ratio between the two ILs
25
26
27 of ~1:1. The exposure of the samples to ambient conditions was extremely minimized.
28
29
30
31 However, an undetermined amount of water was inexorably incorporated to the samples
32
33
34 due to their high hygroscopicity. Visual observations indicated that RadIL and
35
36
37 [BMIm⁺]₂[Cl⁻] [Tos⁻] exhibited liquid characteristics in the entire temperature range of
38
39
40
41 interest. The results obtained in the thermal experiments were not sufficiently conclusive
42
43
44 to determine whether they are supercooled liquids or mixtures with broad melting points
45
46
47 affected by the amount of water present (see Supporting Information for details). A more
48
49
50
51
52
53
54
55
56
57
58
59
60 exhaustive physicochemical characterization of ILs, including X-ray and rheology

1
2
3 techniques, could help to discard phase segregations and understand the fluid behavior
4
5
6
7 of the materials.
8
9

10
11 Aqueous solutions of [BMIm⁺][Cl⁻] and [H⁺][Tos⁻] were prepared for the spectroscopic
12
13
14
15 measurements using deionized water (18 MΩ × cm, obtained from a Milli-Q system).
16
17

18 Solutions were kept under darkness for 24 hours before use.
19
20
21

22
23 *Spectroscopic measurements.* Absorption measurements were performed in a Cary
24
25
26 50 Conc UV-vis spectrophotometer (Varian), equipped with a thermostated sample-
27
28
29 holder. The bandwidth of the excitation slit was 1.5 nm. Depending on the optical
30
31
32 densities of the samples, quartz cells of different optical path-lengths were used. A 0.2
33
34
35 cm optical path was used for the following samples: a blend of 2.2×10^{-4} M of
36
37
38 [BMIm⁺][HPTS³⁻] in [BMIm⁺][Cl⁻], RadIL and diluted aqueous solutions of [BMIm⁺][Cl⁻]
39
40
41 and [H⁺][Tos⁻]. On the other hand, a 10 μm optical path was used for [BMIm⁺]₂[Cl⁻]
42
43
44 [Tos⁻] and the concentrated aqueous solution of [H⁺][Tos⁻].
45
46
47
48
49
50

51
52 Steady-state fluorescence spectra were recorded in a PTI QuantaMaster 4 CW
53
54
55 fluorometer, equipped with a xenon short-arc lamp UXL-75XE and a thermostated
56
57
58
59
60

1
2
3 sample-holder. Both excitation and emission monochromators have gratings of 1200
4
5
6
7 line/mm, in which 1 mm corresponds to a bandwidth of 4 nm. The excitation and
8
9
10 emission slits were adjusted to a bandwidth of 1.5 nm. Diluted samples were measured
11
12
13
14 in a right-angle configuration using a quartz cell of 1 cm optical path-length.
15
16

17 Concentrated highly absorbing samples were measured in transmission geometry using
18
19
20 quartz cells of 0.2 cm and 10 μm optical path-lengths and 1 cm width to minimize inner-
21
22
23
24 filter effects. The optical paths used for the different samples were the same as those
25
26
27
28 mentioned above for absorbance measurements. The commercial spectrofluorometer
29
30
31 was adapted to a transmission configuration in which the fluorescence was collected at
32
33
34
35 180° with respect to the excitation beam.²⁰ An Asahi™ BP260 filter was interposed
36
37
38
39 between the excitation source and the sample in $[\text{Tos}^-]$ fluorescence acquisitions, to
40
41
42 minimize any spurious excitation light of higher wavelengths from reaching the sample.
43
44

45 A Schott UG11 was used to fulfill this requirement in both $[\text{HPTS}^{3-}]$ and RadIL
46
47
48
49 determinations. For the last two cases, a Schott WG360 filter was also placed between
50
51
52
53 the sample and the detector to avoid the excitation light from reaching the detector. The
54
55
56
57 blank was subtracted in each spectrum, and the experimental data were properly
58
59
60

corrected using the emission corrective function provided by the manufacturer. All measurements were performed at $(20.0 \pm 0.1) ^\circ\text{C}$, except those in which the temperature was the variable of interest.

The fluorescence quantum yield (Φ_F) of $[\text{BMIm}^+]_2[\text{Cl}^-][\text{Tos}^-]$ in water was determined in transmission configuration at $20.0 \pm 0.1 ^\circ\text{C}$ relative to a reference, according to the following expression:

$$\Phi_F = \Phi_{F,R} \frac{n^2}{n_R^2} \frac{f_R(\lambda_0)}{f(\lambda_0)} \frac{\int_{\lambda} L_P(\lambda_0, \lambda) d\lambda}{\int_{\lambda} L_{P,R}(\lambda_0, \lambda) d\lambda} \quad (1)$$

where n represents the refraction index, $f(\lambda_0)$ the absorption factor and $L_P(\lambda_0, \lambda)$ the spectral photon irradiance, and the R subscript denotes reference values. A value of 0.059 ± 0.005 was obtained by using a 0.1 M aqueous solution of $[\text{H}^+][\text{Tos}^-]$ in water as reference ($n_D = 1.3323$, $\Phi_F [\text{H}^+][\text{Tos}^-] = 0.055 \pm 0.015$). The values of Φ_F at different temperatures were referred to those obtained at 20° . The concentrated reference solution of $[\text{H}^+][\text{Tos}^-]$ has the same Φ_F as a diluted solution of 1.5×10^{-4} M of the same compound, showing no evidence of excimer formation (data not shown). The relative

1
2
3 determination of Φ_F for this diluted sample was obtained by using a solution of 1.6×10^{-4}
4 M of toluene (Fluka, puriss. p.a. ACS; > 99.7% CG) in degassed cyclohexane (Merk,
5
6
7 Uvasol® for spectroscopy) as reference ($n_D = 1.4233$, Φ_F (toluene/cyclohexane) = 0.14
8
9
10
11 ± 0.02).²¹ In this case, the fluorescence spectra of the diluted samples were acquired in
12
13
14 a 90° configuration using a quartz cell of 1 cm optical path.
15
16
17
18
19
20
21

22 *Refraction indexes measurements.* The refractive indexes of samples were measured
23
24
25 at 589.3 nm in a thermostated Abbemat 300™ automatic refractometer (Anton Paar).
26
27
28
29

30 *Thermal analysis.* DSC and thermogravimetric analysis (TGA) were carried out with a
31
32
33 SDT Q600 V20.9 equipment (TA Instruments). A ramp temperature of 10.00 °C/min was
34
35
36 used until reaching 350.00 °C. Endothermic processes were recorded as downward
37
38
39 peaks. The samples were dried in a vacuum oven at 100 °C for about 12 hours and
40
41
42 subsequently cooled to -20°C during a week before use.
43
44
45
46
47

48 *Liquid scintillation measurements.* Scintillation measurements were performed in a
49
50
51 designed home-made system composed of two Burle 8850 photomultiplier tubes
52
53
54 arranged at 180 degrees, working in coincidence, at both sides of a thermostated
55
56
57
58
59
60

sample holder. The electronic noise was drastically reduced by only computing events in coincidences within 50 μs temporal windows between the signals generated by both photomultiplier tubes. A few drops ($\sim 10\text{-}40\ \mu\text{l}$) of three standardized radioactive aqueous solutions, with a total activity between 5 and 20 kBq, were added into three different standard 5 ml-cylinder glass vials containing 3.2 ml of RadIL (see Supporting Information for details). Two of these sources were prepared using the pure beta emitters ^{14}C and ^{32}P , and the third one with the alpha emitter, ^{241}Am . The maximum energy of the particles emitted by these radionuclides and its Cherenkov threshold energy in ILs are listed in Table 1.

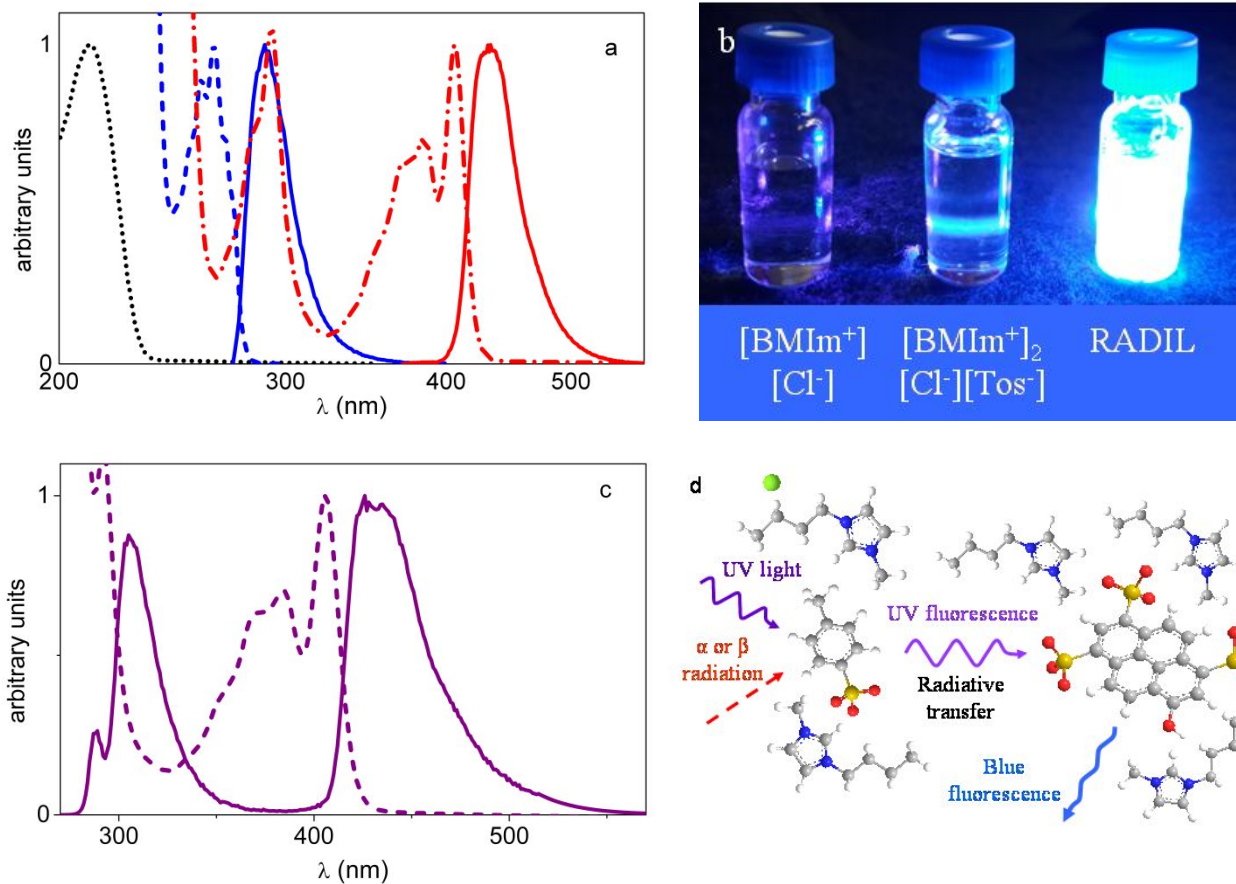
Radionuclide	^{14}C	^{241}Am	^{32}P
Decay	β^-	α	β^-
$E_{\text{max}}(\text{keV})$	~ 156	~ 5570	~ 1711
$E_{\text{thr}}(\text{keV})$	~ 165	$\sim 1.2 \times 10^6$	~ 165
Cherenkov	No	No	Yes

Table 1. Types of decay, maximum energy of the emitted particles and Cherenkov energy threshold in ILs (calculated from $n = 1.53$) for each radionuclide.

RESULTS AND DISCUSSION

The RadIL components fulfill different functions: a) $[\text{Tos}^-]$ anions act as excitation energy harvesters, b) $[\text{BMIm}^+][\text{Cl}^-]$ preclude solidification of the material at the working temperatures and; c) $[\text{HPTS}^{3-}]$ anions serve as emission wavelength shifters. Figure 1a shows the normalized absorption and fluorescence spectra of the RadIL constitutive ions. The absorption and fluorescence spectra of $[\text{BMIm}^+]_2[\text{Cl}^-][\text{Tos}^-]$ resembles those of the monomeric species obtained in a diluted aqueous solution of $[\text{H}^+][\text{Tos}^-]$ (See Supporting Information). Despite the extremely high fluorophore concentration of $\sim 2\text{M}$ in the IL, no aggregates were observed neither in the ground nor in the excited states. The high viscosity combined with the strength of the ionic interactions in the $[\text{BMIm}^+]_2[\text{Cl}^-][\text{Tos}^-]$ would seem to be sufficient to prevent aggregation. The singular presence of the monomer spectra causes an effective overlap between $[\text{Tos}^-]$ emission and $[\text{HPTS}^{3-}]$ absorption, ensuring a suitable energy transfer in the designed material. The addition of $[\text{Tos}^-]$ and $[\text{HPTS}^{3-}]$ to $[\text{BMIm}^+][\text{Cl}^-]$ causes the blue fluorescence of the

liquid observed in Figure 1b. As such, the composition of RadIL maximizes the emission at 420 nm, which corresponds to the wavelength of maximum cathode sensitivity of many commercial photomultipliers,²² for standard 5 ml-cylinder scintillation glass vials.



1
2
3
4 **Figure 1.** a) Normalized absorption and emission spectra of RadIL constitutive ions:
5
6
7 [BMIm⁺][Cl⁻] in water (dotted black line), [BMIm⁺]₂[Cl⁻] [Tos⁻] (dashed and solid blue
8
9
10 lines, by exciting at $\lambda_{\text{exc}} = 260$ nm) and [BMIm⁺][HPTS³⁻] in [BMIm⁺][Cl⁻] (dotted-dashed
11
12
13 and solid red lines, by exciting at $\lambda_{\text{exc}} = 345$ nm) ; b) Fluorescence from [BMIm⁺][Cl⁻],
14
15
16 [BMIm⁺]₂[Cl⁻] [Tos⁻] and RadIL, using $\lambda_{\text{exc}} = 400$ nm. c) Normalized absorption (dashed
17
18
19 violet line) and fluorescence (solid violet line) spectra of RadIL, measured in
20
21
22 transmission geometry with an optical path-length of 0.2 cm at $\lambda_{\text{exc}} = 260$ nm. d)
23
24
25
26
27
28 Scheme representing the vibronic molecular excitation of [Tos⁻] by UV-light or energetic
29
30
31 charged particles, followed by radiative energy transfer to the [HPTS³⁻] and the final
32
33
34
35 emission of blue photons with a maximum around 420 nm.
36
37
38
39
40
41
42
43

44 The absorption and the emission spectra of the RadIL are presented in Figure 1c.
45
46
47 Note that both, the fluorescence maximum located at 435nm and the value of 1.9
48
49
50
51 obtained for the ratio between the maximum absorbance at 406 nm and the first
52
53
54
55 minimum towards the blue at 394 nm, are clear indicators that the polarity of the
56
57
58
59
60

1
2
3 surrounding media of [HPTS³⁻] differs from those observed for the same fluorophore in
4
5
6
7 3M hydrochloric acid aqueous solution.²³
8
9

10
11 The scheme presented in Figure 1d depicts the excitation energy transfer
12
13 mechanisms taking place in the RadIL. Upon vibronic excitation of [Tos⁻] by the UV-light
14
15 or by energetic charged particles, the excitation energy is radiatively transferred to
16
17
18 [HPTS³⁻] and finally emitted as blue photons, which mostly escape out of the system.
19
20
21
22
23
24
25

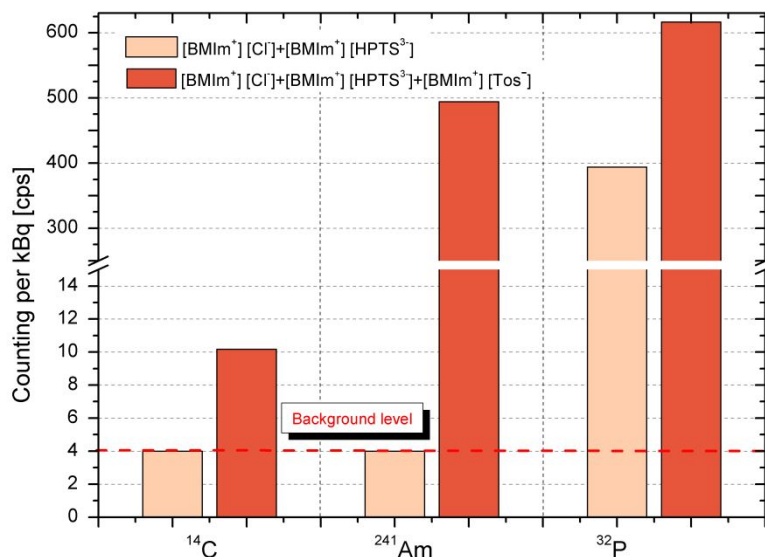
26 Fluorescence and radioluminescence are not the only phenomena that can be
27
28 promoted in the RadIL environments. Cherenkov radiation is also generated when
29
30 charged particles travel faster than the speed of light in that medium. This light can be
31
32
33 further re-absorbed by [HPTS³⁻] and finally emitted as blue fluorescence photons as
34
35
36
37 well,¹⁷ contributing to the total signal emerging from the material. Note that the
38
39
40 Cherenkov light is actually not included in the current definition of radioluminescence²⁴
41
42
43 since it originates from neither excited electronic nor vibrational molecular states.²⁵
44
45
46
47
48
49
50

51 The RadIL capability to convert the energy released by energetic particles into visible
52
53 light was tested by adding different radionuclide solutions to this material. As such, the
54
55
56
57
58
59
60

1
2
3 rate of photon bunches emerging from vials containing ^{14}C , ^{241}Am and ^{32}P was
4
5
6
7 determined by liquid scintillation counting (LSC). The main advantage of LSC, in
8
9
10
11 contraposition with other techniques, is its high geometric efficiency since both
12
13
14 scintillation and radioactive material are mixed in the same volume. Figure 2
15
16
17 summarizes the results obtained by measuring the counting in temporal coincidence,
18
19
20
21 normalized by the activity, for the three prepared radioactive sources plus a vial with
22
23
24 pure RadIL, used as a blank for background determination. All experiments were
25
26
27 performed at 20°C . The figure also includes three results obtained by dissolving ^{14}C ,
28
29
30
31 ^{241}Am and ^{32}P in $[\text{BMIm}^+][\text{Cl}^-]$ plus 2.2×10^{-4} M of $[\text{BMIm}^+][\text{HPTS}^{3-}]$ as a reference for
32
33
34
35 Cherenkov detection.

36
37
38
39 Emissions from ^{14}C and ^{241}Am do not yield Cherenkov radiation in the ILs since
40
41
42
43 neither the electrons emitted by ^{14}C nor the alpha particles emitted by ^{241}Am , nor Auger
44
45
46 and conversion electrons have enough energy to reach the Cherenkov threshold. In
47
48
49
50 fact, only background signals are obtained for ^{14}C and ^{241}Am in the ILs when $[\text{Tos}^-]$ is
51
52
53
54 absent. However, the same radionuclides produce a double coincidence counting
55
56
57
58
59
60

1
2
3 significantly above the background when they are dissolved in the RadIL. Since ^{14}C is a
4
5
6
7 pure beta emitter and there is a negligible probability of photon emission with energies
8
9
10 above the threshold energy by ^{241}Am , such an observation can be undoubtedly be
11
12
13 attributed to the radioluminescence phenomena. The contribution from direct interaction
14
15
16 of X-ray or gamma photons to the photocathode was safely discarded after verifying
17
18
19 that the interposing a dark paper in between the vial and the detector reduced the
20
21
22 double counting below the background level. On the other hand, the free electrons that
23
24
25 could eventually be originated in the RadIL by photoelectric or Compton effects should
26
27
28 not exceed the Cherenkov threshold.
29
30
31
32
33
34
35
36
37
38
39
40
41
42
43
44
45
46
47
48
49
50
51
52
53
54
55
56
57
58
59
60



1
2
3
4
5
6
7
8
9
10
11
12 **Figure 2.** Coincidence counting per kBq of activity obtained in [BMIm⁺][Cl⁻] +
13
14
15 [BMIm⁺][HPTS³⁻] (light yellow bars) and RadIL ([BMIm⁺][Cl⁻] + [BMIm⁺][HPTS³⁻] +
16
17
18 [BMIm⁺][Tos⁻]) (orange bars) for the three radionuclides used in this work. All
19
20
21
22
23 measurements were performed at 20 Celsius degrees.
24
25
26
27
28
29
30

31
32 Contrasting with the ¹⁴C, and the ²⁴¹Am cases, the electrons emitted by ³²P did
33
34
35 generate Cherenkov photons in the ILs,¹⁷ since a part of its beta spectrum is above the
36
37
38 Cherenkov threshold. Besides, when ³²P was dissolved in the RadIL, the double
39
40
41 coincidence counting was significantly higher than the one obtained in [BMIm⁺][Cl⁻] plus
42
43
44 2.2×10^{-4} M of [BMIm⁺][HPTS³⁻]. This improvement could be attributed, in principle, to
45
46
47 the absorption of Cherenkov light by [Tos⁻] ions, followed by a subsequent emission,
48
49
50
51
52
53 which enables for [HPTS³⁻] to shift the luminescence towards the red. However, since
54
55
56
57
58
59
60

1
2
3 the electrons from ^{14}C do produce radioluminescence, there is no reason why those
4
5
6
7 from ^{32}P – one order of magnitude more energetic on average – would not. Both
8
9
10 radionuclides are pure beta emitters, i.e., no other particles except electrons (and the
11
12
13 elusive antineutrinos) come out from its nuclei. Hence, as in the former case, this
14
15
16
17 enhancement can also be attributed – at least partially – to the radioluminescence
18
19
20
21 phenomena. As will be shown below, the eventual contribution of the red-shifted
22
23
24 Cherenkov emission is not significant compared to radioluminescence.
25
26
27
28

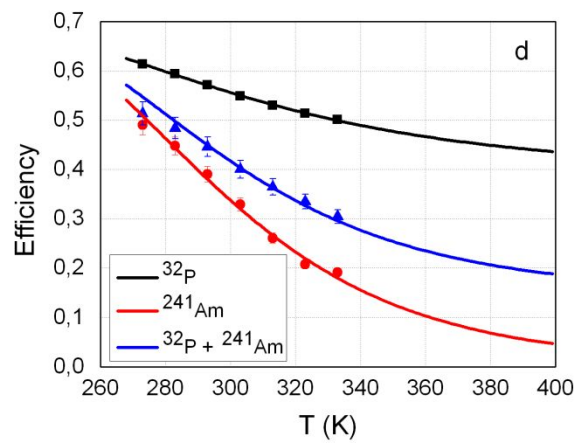
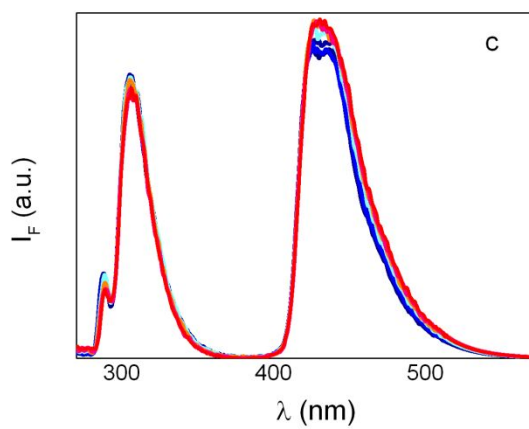
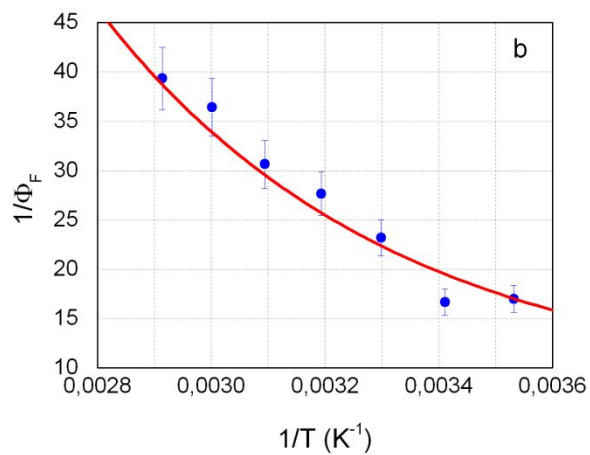
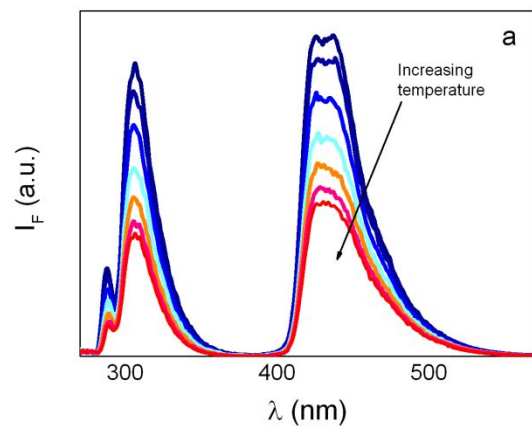
29 A keynote of the RadIL radioluminescence is its change in the emission intensity with
30
31
32 temperature. The fluorescence of RadIL decreases significantly as the temperature
33
34
35 increases, as it is shown in Figure 3a. This behavior can be attributed to the
36
37
38
39 fluorescence quenching of $[\text{Tos}^-]$ with temperature. The trend of Φ_{F} of
40
41
42 $[\text{BMIm}^+]_2[\text{Cl}^-][\text{Tos}^-]$ as a function of temperature depicted in Figure 3b supports this
43
44
45
46 statement. In addition, a similar tendency is observed for the Φ_{F} of $[\text{H}^+][\text{Tos}^-]$ in diluted
47
48
49 aqueous solution (data not shown). Although the fluorescence intensity of $[\text{HPTS}^{3-}]$ also
50
51
52
53 changes with temperature, it does in a significantly lesser extent, as it can be seen in
54
55
56
57
58
59
60

1
2
3 Figure 3c where it is shown the fluorescence spectra of RadIL at different temperatures
4
5
6
7 normalized to 310 nm, the maximum of $[\text{Tos}^-]$ emission. Therefore, as mentioned
8
9
10 before, all these arguments strongly support that the number of photons radiatively
11
12
13 transferred from $[\text{Tos}^-]$ to $[\text{HPTS}^{3-}]$ diminishes with temperature due to the decrease in
14
15
16
17 $[\text{Tos}^-]$ fluorescence.
18
19
20
21

22 The above-mentioned fluorescence temperature dependence is translated into
23
24
25 changes in the detection efficiency (expressed in terms of the experimental double
26
27
28 coincidence counts over the activity) when the sources, prepared using RadIL as a
29
30
31 solvent, are measured by LCS. We remark that the lower the mean number of
32
33
34 radioluminescent photons is, the lower the probability of coincidences. Note that this
35
36
37 behavior is incompatible with both Cherenkov radiation and direct interaction of X or
38
39
40 gamma photons with the photocathode, reinforcing the argument raised before about
41
42
43 the nature of the photons emitted by the RadIL. This feature also constitutes a
44
45
46
47 significant difference compared with all available commercial scintillation cocktails. The
48
49
50 organic solvents present in these preparations are volatile and flammable, precluding
51
52
53
54
55
56
57
58
59
60

1
2
3 the heating of the radioactive sources. On the other hand, the ionic nature of RadIL
4
5
6
7 avoids evaporation losses and flammability risks by warming.
8
9

10
11 Figure 3d shows the efficiencies of double temporal coincidences in the activity
12
13
14
15 determination of three radioactive sources at different temperatures. As before, the
16
17
18 sources were ^{241}Am and ^{32}P , and an extra sample consisting of a mixture of both
19
20
21
22 radionuclides as well. It is observed that the efficiency always decreases as
23
24
25 temperature increases, although shows different trends in each particular case.
26
27
28
29
30
31
32
33
34
35
36
37
38
39
40
41
42
43
44
45
46
47
48
49
50
51
52
53
54
55
56
57
58
59
60



1
2
3 **Figure 3.** a) Temperature fluorescence dependence of RadIL, measured at $\lambda_{\text{exc}} = 260$
4 nm in transmission geometry with an optical path-length of 0.2 cm; b) temperature
5
6
7 dependence of [BMIm⁺]₂[Cl⁻][Tos⁻] fluorescence quantum yield at $\lambda_{\text{exc}} = 260$ nm; c)
8
9
10
11
12
13
14 Normalized spectra of Item a at 310 nm, the maximum of [Tos⁻] emission; and d)
15
16
17
18 Experimental efficiencies of double coincidences for ²⁴¹Am (red circles), ³²P (black
19
20
21 squares) and a mixture of both radionuclides (blue triangles) as a function of
22
23
24 temperature. The solid lines represent the simulated efficiencies.
25
26
27
28
29
30
31
32

33
34 A simplified description for the probability of double coincidences produced by an
35
36
37 alpha emitter, $\varepsilon_{\alpha}(T)$, can be achieved by expressing it as a function of the mean
38
39
40
41 number of emitted photons, m :
42
43
44

$$\varepsilon_{\alpha}(T) = \left[1 - e^{-V_{\alpha} \cdot m}\right]^2 \quad (2)$$

45
46
47
48
49
50 where V_{α} is a parameter that depends on the quantum efficiency of photomultipliers,
51
52
53
54 among many other characteristics of the detection system.²⁶ The charge, energy and
55
56
57
58
59
60

1
2
3 mass of ionizing particles determine the density of individual molecular excitations and
4
5
6
7 ionizations. The local density of excited and ionized ions created by electrons is lower
8
9
10 than those created by alpha particles of the same energy. The scintillation response is
11
12
13 then practically proportional to the particle's energy when it is produced by electrons,
14
15
16 while being roughly constant when it is produced by alpha particles.²² Therefore,
17
18
19
20
21 Equation 2 remains valid – to a good approximation – for alpha particles without adding
22
23
24 more information about the decay.
25
26
27
28

29 A temperature dependence of the expression in Equation 2 can be obtained if m is
30
31
32 written as a function of the same parameters describing the above-mentioned
33
34
35 fluorescence temperature behavior of the RadIL (see Supporting Information). The
36
37
38 results shown in Fig. 3d reveal that the model reproduces the observed trend for ²⁴¹Am.
39
40
41
42
43 In particular, the efficiency diminishes as the temperature is raised and is controlled by
44
45
46 the radiative rate-constant (k_F) and the temperature independent non-radiative rate-
47
48
49 constant (k_{nr}^0) of [Tos⁻].
50
51
52
53
54
55
56
57
58
59
60

1
2
3
4 On the other hand, compared to the ^{241}Am results, the temperature dependence of the
5
6
7 efficiency for ^{32}P looks milder. Although the radioluminescent photons are strongly
8
9
10 quenched at such conditions, the Cherenkov radiation still remains present. The
11
12
13 refraction index of ILs only suffers very small changes with temperature (See
14
15
16 Supporting Information), while the Cherenkov intensity remains fairly constant. As such,
17
18
19 the efficiency of double temporal coincidence produced by both radioluminescent and
20
21
22 Cherenkov photons after a beta decay, $\varepsilon_{\beta+Ch}(T)$, can be described according to the
23
24
25 following expression:
26
27
28
29
30
31

$$\varepsilon_{\beta+Ch}(T) = \int_0^E N(E') \cdot \left(1 - e^{-[\nu_{\beta} \cdot m(E') + \nu_{Ch} \cdot k(E')]}\right)^2 dE' \quad (3)$$

32
33
34 where E is the energy, $N(E')$ is the spectrum of the beta particles, $k(E')$ is the number
35
36
37 of Cherenkov photons, and ν_{β} and ν_{Ch} are two fitting adjustable parameters.²⁷ Note
38
39
40 that $m(E')$ here is explicitly considered as a function of the energy.
41
42
43
44
45
46
47
48
49
50

51 Equation 3 describes satisfactory the observed trend for ^{32}P shown in Figure 3d, when
52
53
54 $m(E')$ is written as a function of the temperature by using the same parameters
55
56
57
58
59
60

1
2
3 describing the fluorescence temperature behavior of the RadIL (see Supporting
4
5
6
7 Information).

8
9
10
11 The efficiency of the ^{241}Am and ^{32}P mixture, $\varepsilon_M(T)$, remains intermediate between the
12
13
14 efficiency values of the individual radionuclides. Figure 3d shows $\varepsilon_M(T)$ as a function of
15
16
17 temperature, obtained by a linear fitting of a combination of the efficiencies of each
18
19
20
21 radionuclide weighted by their activities. As a result, a good agreement between the
22
23
24 activities used to adjust the efficiency of the mixture and the activity of each radionuclide
25
26
27
28 separately was found. This example clearly illustrates the use of the RadIL for α/β
29
30
31
32 quantification after pre-calibration of the material response to each radionuclide present
33
34
35
36 in the mixture.

37 38 39 40 CONCLUSIONS

41
42
43
44 A radioluminescent IL was successfully synthesized, aiming at representing the
45
46
47 starting point in the research of new non-volatile liquids materials for detecting and
48
49
50
51
52 quantifying ionizing radiation. The RadIL obtained in this work was specially designed to
53
54
55
56 gather different anions to adequately modulate the radiative energy transfer
57
58
59
60

1
2
3 phenomenon to ensure an effective conversion of the excitation energy into visible
4
5
6
7 emission. The efficiency of the present material is not yet comparable with those from
8
9
10 commercial cocktails, but further research in the area is carried out to improve this
11
12
13 aspect. The keynote of this material is the temperature dependence of the
14
15
16 radioluminescence. This feature was proved to be used for alpha/beta quantification in
17
18
19 radionuclide mixtures, following a pre-calibration of the material.
20
21
22
23
24

25 In general, the use of radioluminescent ionic liquids provide several improvements
26
27
28 with respect to the commercial cocktails; without begin exhaustive, the following list
29
30
31 includes some relevant examples:
32
33
34
35
36

37 a) They provide customized solubilities for radioactive compounds, especially
38
39
40 considering that they can be designed with tailored properties. Regarding solubility, they
41
42
43 also hold up higher amounts of water compared to many commercial cocktails, which
44
45
46 generally form emulsions that hinder scintillation measurements upon the incorporation
47
48
49 of minimum contents of aqueous solutions.
50
51
52
53
54
55
56
57
58
59
60

1
2
3
4 b) Secondly, an interesting advantage is the possibility of repeatedly performing
5
6
7 heating-cooling cycles without evidencing of evaporation losses or flammability risks.
8

9
10 This makes possible to implement a safe temperature control when they are used as
11
12
13 solvent for radioactive sources. This property also offers an alternative method for
14
15
16 efficiency determination in very accurate and absolute LSC techniques as CIEMAT-
17
18 NIST²⁸ and Triple to Double Coincidences Ratio (TDCR), by using the temperature as a
19
20
21 quenching parameter.
22
23
24
25

26
27
28
29 c) They can also be re-used after removing aqueous solutions residues by simple
30
31
32 evaporation in a vacuum oven when short-lived radionuclides are measured. Of course,
33
34
35 the great stability of the ILs opens the possibility to implement several techniques based
36
37
38 on solvent extraction to separate the radioactive analytes and followed by the recovery
39
40
41 and reuse of the material. Their special properties also make this novel material suitable
42
43
44 for real-time quantification of the yielding achieved by solvent extraction of lanthanides,
45
46
47 actinides, and fission products into IL solutions during nuclear fuel reprocessing. The
48
49
50
51
52
53
54
55
56
57
58
59
60

1
2
3 research on these interesting and complex areas, with several potential applications,
4
5
6
7 represents a present challenge worth pursuing.
8
9

10
11 d) They usually have high refractive indexes and therefore lower Cherenkov
12
13 thresholds compared to water. For instance, for the ^{18}F radionuclide, its implementation
14
15 yields a 100% enhancement in the detection efficiency.¹⁶
16
17
18
19

20
21 e) The ionic interactions prevailing in the ILs along with the high viscosity seem to
22
23 prevent the aggregation of species both in the fundamental and excited states, even at
24
25 extremely high local chromophore concentrations. In this sense, the proper
26
27 management of the size of the alkyl substituents could be a suitable tool to modulate
28
29 the appearance of these species, similarly to what has already been reported for
30
31 molecular liquids.^{29,30} Besides, the adequate selection of the constitutive ions and the
32
33 tuning of their emission spectra allow the quest for an efficient energy transfer between
34
35 donors and acceptors to achieve a highlighted fluorescence in the spectral region of
36
37
38
39
40
41
42
43
44
45
46
47
48
49
50
51 interest.
52
53
54
55
56
57
58
59
60

1
2
3 f) Fluorophores incorporated into ILs are generally exposed to lower extents of oxygen
4
5
6
7 quenching compared with organic solvents. This fact improves the quantum efficiency
8
9
10 and the optical stability of these liquid materials.³¹
11
12
13

14
15 The previous considerations provide clear evidence of a paramount of applications of
16
17
18 radioluminescent ionic liquids beyond the detection and quantification of ionizing
19
20
21
22 radiation, especially in those applications in which excitation energy, regardless of its
23
24
25 nature, must be efficiently manageable.
26
27
28

29 ASSOCIATED CONTENT

30
31
32
33
34 **Supporting Information.** A theoretical approach describing the temperature dependence
35
36
37 of efficiencies is presented. The refraction index data of RadIL as a function of
38
39
40 temperature, the characteristics of the standardized sources, DCS and TGA results, and
41
42
43 absorption and fluorescence spectra of $[\text{BMIm}^+]_2[\text{Cl}^-][\text{Tos}^-]$ and $[\text{H}^+][\text{Tos}^-]$ aqueous
44
45
46 solutions are also included. The following file is available free of charge.
47
48
49

50
51
52 RADIL_SI.pdf
53
54
55
56
57
58
59
60

1
2
3
4 AUTHOR INFORMATION
5
6

7
8 **Corresponding Authors**
9

10
11 *E-mail: dariorodrigues@cnea.gov.ar; mirenda@cnea.gov.ar
12
13

14
15
16 ORCID
17

18
19 Dario Rodríguez: 0000-0002-7952-7168
20
21

22
23 Gabriela P. Sarmiento: 0000-0001-5945-9359
24
25

26
27 Nicolás I. Krimer: 0000-0003-0261-827X
28
29

30
31 Martín Mirenda: 0000-0003-0478-5178
32

33
34 **Author Contributions**
35
36

37
38 G.P.S. and N.I.K. synthesized, purified and characterized the ILs. N.I.K. and D.R.
39

40
41 performed the fluorescence measurements. D.R. built the home-made scintillation
42

43
44 system and carried out the scintillation experiments. D.R. and M.M. performed the
45

46
47 analysis of experimental data. M.M. proposed the original idea of ILs as scintillation
48

49
50 solvents. D.R. discovered the radioluminescence temperature dependence of RadIL. All
51
52
53
54
55
56
57
58
59
60

1
2
3 authors contributed to the discussion of the results and writing of the manuscript. D.R.

4
5
6
7 and M.M. are the corresponding authors.
8
9

10 11 **Funding Sources** 12

13
14
15 M.M. and N.I.K. received funding from CONICET (PIP 11220130100795CO). D.R.,

16
17
18 M.M. and N.I.K. received funding from ANPCyT (PICT2018-02153).
19
20
21
22
23
24
25

26 27 **ACKNOWLEDGMENT** 28

29
30 G.P.S. had a postdoctoral fellowship from CNEA. N.I.K. is a staff member of CNEA.
31
32

33
34 D.R. is a staff member of CONICET. M.M. is a staff member of CNEA and CONICET.
35
36

37 Authors thank Gabriela Cerruti and María Clara Ferrari for kindly support for sample
38
39
40 preparations. Authors also acknowledge Pablo Arenillas, Christian Balpardo and Eliana
41
42
43

44 Depaoli for providing the physical space to perform the scintillation measurements.
45
46

47 Authors would like to express special thanks to Maria Laura Japas for her standing
48
49

50
51 support, Maria Gabriela Lagorio for your kindly help in imaging processing and Daniel
52
53
54
55
56
57
58
59
60

1
2
3 Laria for the further discussion of the manuscript. MM thanks to Dr. Pablo Maggi for his
4
5
6
7 positive and effective intervention that made a prompt recovery possible.
8
9
10
11
12
13
14

15 REFERENCES

16
17
18
19
20
21

- 22 (1) Welton, T. Ionic Liquids: a Brief History. *Biophys. Rev.* **2018**, *10*, 691–706.
23
24
25
26 (2) Egorova, K. S.; Gordeev, E. G.; Ananikov, V. P. Biological Activity of Ionic
27
28
29
30 Liquids and their Application in Pharmaceuticals and Medicine. *Chem. Rev.* **2017**, *117*,
31
32
33 7132–7189.
34
35
36
37 (3) Cao, Y.; Tan, Y. J.; Li, S.; Lee, W. W.; Guo, H.; Cai, Y.; Wang, C.; Tee, B. C.-K.
38
39
40
41 Self-healing Electronic Skins for Aquatic Environments. *Nat. Electron.* **2019**, *2*, 75–82.
42
43
44
45 (4) Watanabe, M.; Thomas, M. L.; Zhang, S.; Ueno, K.; Yasuda, Y.; Dokko, K.
46
47
48
49 Application of Ionic Liquids to Energy Storage and Conversion Materials and Devices.
50
51
52
53 *Chem. Rev.* **2017**, *117*, 7190–7239.
54
55
56
57
58
59
60

- 1
2
3
4 (5) Smiglak, M.; Pringle, J. M.; Lu, X.; Han, L.; Zhang, S.; Gao, H.; MacFarlane, D.
5
6
7 R.; Rogers, R. Ionic Liquids for Energy, Materials, and Medicine. *Chem. Commun.*
8
9
10 **2014**, *50*, 9228–9250.
11
12
13
14
15 (6) Barna, V.; De Cola, L. Mirrorless Dye Doped Ionic Liquid Lasers. *Opt. Express*
16
17
18 **2015**, *23*, 11936–11945.
19
20
21
22
23 (7) Sun, X.; Luo, H.; Dai, S. Ionic Liquids-based Extraction: a Promising Strategy for
24
25
26 the Advanced Nuclear Fuel Cycle. *Chem. Rev.* **2012**, *112*, 2100–2128.
27
28
29
30
31 (8) Straka, M. Toward a Greenish Nuclear Fuel Cycle: Ionic Liquids as Solvents for
32
33
34 Spent Nuclear Fuel Reprocessing and Other Decontamination Processes for
35
36
37 Contaminated Metal Waste. *Phys. Sci. Rev.* **2016**, *1*, 20160074.
38
39
40
41
42 (9) Rogers, R. D.; Seddon, K. R. Ionic Liquids-Solvents of the Future. *Science* **2003**,
43
44
45 *302*, 792–793.
46
47
48
49
50 (10) Freemantle, M. *An Introduction to Ionic Liquids*; RSC Publishing: Cambridge, UK,
51
52
53 **2010**.
54
55
56
57
58
59
60

1
2
3
4 (11) Shi, R.; Wang, Y. Dual Ionic and Organic Nature of Ionic Liquids. *Sci. Rep.* **2016**,
5
6
7 *6*, 19644.
8
9

10
11 (12) Mohapatra, P. K. Actinide Ion Extraction Using Room Temperature Ionic Liquids:
12
13
14 Opportunities and Challenges for Nuclear Fuel Cycle Applications. *Dalton Trans.* **2017**,
15
16
17
18 *46*, 1730–1747.
19
20

21
22 (13) Ha, S. H.; Menchavez, R. N.; Koo, Y-M. Reprocessing of Spent Nuclear Waste
23
24
25
26 Using Ionic Liquids. *Korean J. Chem. Eng.* **2010**, *27*, 1360–1365.
27
28

29
30 (14) Mincher, B. J.; Wishart, J. F. The Radiation Chemistry of Ionic Liquids: A Review.
31
32
33
34 Solvent Extr. Ion Exc. 2014, *32*, 563–583.
35
36

37
38 (15) Bliznyuk, V. N.; Seliman, A. F.; Ishchenko, A. A.; Derevyanko, N. A.; DeVol, T. A.
39
40
41
42 New Efficient Organic Scintillators Derived from Pyrazoline. *ACS Appl. Mater. Interfaces*
43
44
45
46 **2016**, *8*, 12843–12851.
47
48
49
50
51
52
53
54
55
56
57
58
59
60

1
2
3
4 (16) Mirenda, M.; Rodrigues, D.; Arenillas, P.; Gutkowski, K. Ionic Liquids as Solvents
5
6
7 for Liquid Scintillation Technology. Čerenkov Counting with 1-Butyl-3-Methylimidazolium
8
9
10 Chloride. *Radiat. Phys. Chem.* **2014**, *98*, 98–102.

11
12
13
14
15 (17) Mirenda, M.; Rodrigues, D.; Ferreyra, C.; Arenillas, P.; Sarmiento, G. P.; Krimer,
16
17
18 N. I.; Japas, M. L. Ionic Liquids as Solvents for Čerenkov Counting and the Effect of a
19
20
21 Wavelength Shifter. *Appl. Radiat. Isot.* **2018**, *134*, 275–279.

22
23
24
25
26 (18) Sarmiento, G. P.; Zelcer, A.; Espinosa, M.; Babay, P.; Mirenda, M.
27
28
29
30 Photochemistry of Imidazolium Cations. Water Addition to Methylimidazolium Ring
31
32
33 Induced by UV Radiation in Aqueous Solution. *J. Photochem. Photobiol. A: Chem.*
34
35
36
37 **2016**, *314*, 155–163.

38
39
40
41 (19) Mirenda, M.; Rodrigues, D.; Sarmiento, G. P.; Krimer, N. I. Argentinean patent
42
43
44
45 on request, INPI Number 20180103091, **2018**.

46
47
48
49 (20) Krimer, N. I.; Rodrigues, D.; Rodríguez, H. B.; Mirenda, M. Steady-state
50
51
52
53 Fluorescence of Highly Absorbing Samples in Transmission Geometry: a Simplified
54
55
56
57
58
59
60

1
2
3
4 Quantitative Approach Considering Reabsorption Events. *Anal. Chem.* **2017**, *89*, 640–
5
6
7 647.

8
9
10
11 (21) Quina, F. H.; Carroll, F. A. Radiative and Nonradiative Transitions in Solution.
12
13
14
15 First Excited Singlet State of Benzene and Its Methyl Derivatives. *J. Am. Chem. Soc.*
16
17
18 **1976**, *98*, 6–9.

19
20
21
22
23 (22) Birks, J. B. *The Theory and Practice of Scintillation Counting*, Pergamon Press:
24
25
26 London **1964**.

27
28
29
30
31 (23) Barrash-Shiftan, N.; Brauer, B. (B.); Pines, E. Solvent Dependence of Pyranine
32
33
34 Fluorescence and UV-visible Absorption Spectra. *J. Phys. Org. Chem.* **1998**, *11*, 743–
35
36
37 750.

38
39
40
41
42 (24) Braslavsky, S. E. Glossary of Terms Used in Photochemistry (3^{er} edition). *Pure*
43
44
45 *Appl. Chem.* **2007**, *79*, 293–465.

46
47
48
49
50 (25) Frank, I. M.; Tamm, I. G. Coherent Visible Radiation of Fast Electrons Passing
51
52
53
54 Through Matter. *Compt. Rend. Acad. Sci. URSS* **1937**, *14*, 109–114.

1
2
3
4 (26) Broda, R.; Cassette, P.; Kossert, K. Radionuclide Metrology Using Liquid
5
6
7 Scintillation Counting. *Metrologia* **2007**, *44*, S36–S52.
8
9

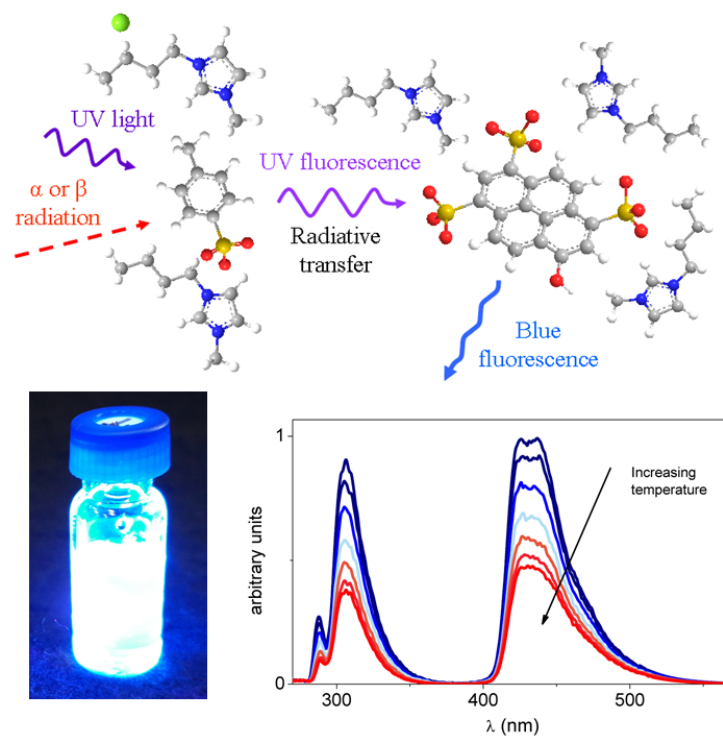
10
11 (27) Kossert, K. Activity Standardization by Means of a New TDCR- Čerenkov
12
13
14
15 Counting Technique. *Appl. Radiat. Isot.* **2010**, *68*, 1116–1120.
16
17
18

19 (28) Grau Malonda, A.; Garcia-Toraño, E. Evaluation of Counting Efficiency in Liquid
20
21
22
23 Scintillation Counting of Pure β -ray Emitters. *Appl. Radiat. Isot.* **1982**, *33*, 249–253.
24
25
26

27 (29) Lu, F.; Nakanishi, T. Solvent-free Luminous Molecular Liquids. *Adv. Optical*
28
29
30
31 *Mater.* **2019**, *7*, 1900176.
32
33
34

35 (30) Lu, F.; Takaya, T.; Iwata, K.; Kawamura, I.; Saeki, A.; Ishii, M.; Nagura, K.;
36
37
38
39 Nakanishi, T. A Guide to Design Functional Molecular Liquids with Tailorable Properties
40
41
42 Using Pyrene-Fluorescence as a Probe. *Sci. Rep.* **2017**, *7*, 3419.
43
44
45

46 (31) Rodriguez, H. B.; Mirenda, M.; Lagorio, M. G.; San Roman, E. Photophysics at
47
48
49
50 Unusually High Dye Concentrations. *Acc. Chem. Res.* **2019**, *52*, 110–118.
51
52
53
54
55
56
57
58
59
60



254x190mm (96 x 96 DPI)